2018-01-22

Analysis of the Human Mucosal Response to Cholera Reveals Sustained Activation of Innate Immune Signaling Pathways

Daniel L. Bourque
Harvard Medical School

Et al.

AMERICAN SOCIETY FOR MICROBIOLOGY | Infection and Immunity®

HOST RESPONSE AND INFLAMMATION

Analysis of the Human Mucosal Response to Cholera Reveals Sustained Activation of Innate Immune Signaling Pathways

Daniel L. Bourque,[a,c] Taufiqur Rahman Bhuiyan,[b] Diane P. Genereux,[e,f] Rasheduzzaman Rashu,[b] Crystal N. Ellis,[a] Fahima Chowdhury,[b] Ashraful I. Khan,[b] Nur Haq Alam,[b] Anik Paul,[b] Lazina Hossain,[b] Leslie M. Mayo-Smith,[a] Richelle C. Charles,[a,c] Ana A. Weil,[a,c] Regina C. LaRocque,[a,c] Stephen B. Calderwood,[a,c,h] Edward T. Ryan,[a,c,g] Elinor K. Karlsson,[e,f] Firdausi Qadri,[b] Jason B. Harris[a,d]

[a]Division of Infectious Diseases, Massachusetts General Hospital, Boston, Massachusetts, USA
[b]International Centre for Diarrhoeal Disease Research, Dhaka, Bangladesh
[c]Department of Medicine, Harvard Medical School, Boston, Massachusetts, USA
[d]Department of Pediatrics, Harvard Medical School, Boston, Massachusetts, USA
[e]Program in Molecular Medicine, University of Massachusetts Medical School, Worcester, Massachusetts, USA
[f]Broad Institute of MIT and Harvard, Cambridge, Massachusetts, USA
[g]Department of Immunology and Infectious Diseases, Harvard T. H. Chan School of Public Health, Boston, Massachusetts, USA
[h]Department of Microbiology and Immunobiology, Harvard Medical School, Boston, Massachusetts, USA

ABSTRACT To better understand the innate immune response to *Vibrio cholerae* infection, we tracked gene expression in the duodenal mucosa of 11 Bangladeshi adults with cholera, using biopsy specimens obtained immediately after rehydration and 30 and 180 days later. We identified differentially expressed genes and performed an analysis to predict differentially regulated pathways and upstream regulators. During acute cholera, there was a broad increase in the expression of genes associated with innate immunity, including activation of the NF-κB, mitogen-activated protein kinase (MAPK), and Toll-like receptor (TLR)-mediated signaling pathways, which, unexpectedly, persisted even 30 days after infection. Focusing on early differences in gene expression, we identified 37 genes that were differentially expressed on days 2 and 30 across the 11 participants. These genes included the endosomal Toll-like receptor gene *TLR8*, which was expressed in lamina propria cells. Underscoring a potential role for endosomal TLR-mediated signaling *in vivo*, our pathway analysis found that interferon regulatory factor 7 and beta 1 and alpha 2 interferons were among the top upstream regulators activated during cholera. Among the innate immune effectors, we found that the gene for DUOX2, an NADPH oxidase involved in the maintenance of intestinal homeostasis, was upregulated in intestinal epithelial cells during cholera. Notably, the observed increases in *DUOX2* and *TLR8* expression were also modeled *in vitro* when Caco-2 or THP-1 cells, respectively, were stimulated with live *V. cholerae* but not with heat-killed organisms or cholera toxin alone. These previously unidentified features of the innate immune response to *V. cholerae* extend our understanding of the mucosal immune signaling pathways and effectors activated *in vivo* following cholera.

KEYWORDS *Vibrio cholerae*, immune mechanisms, mucosal immunity

Vibrio cholerae O1 causes an estimated 3 million cases of cholera and 100,000 deaths per year (1). Despite progress under the Millennium Development Goals in providing access to safe drinking water, the global burden of cholera has increased (1, 2). While infection with *V. cholerae* leads to protection against reinfection for up to 10 years, current vaccines provide more limited protection, especially in children under 5 years of age (3–5). The mechanisms through which infection with *V. cholerae* generates

Received 16 August 2017 **Returned for modification** 7 September 2017 **Accepted** 3 November 2017

Accepted manuscript posted online 13 November 2017

Citation Bourque DL, Bhuiyan TR, Genereux DP, Rashu R, Ellis CN, Chowdhury F, Khan AI, Alam NH, Paul A, Hossain L, Mayo-Smith LM, Charles RC, Weil AA, LaRocque RC, Calderwood SB, Ryan ET, Karlsson EK, Qadri F, Harris JB. 2018. Analysis of the human mucosal response to cholera reveals sustained activation of innate immune signaling pathways. Infect Immun 86:e00594-17. https://doi.org/10.1128/IAI.00594-17.

Editor Manuela Raffatellu, University of California San Diego School of Medicine

Address correspondence to Firdausi Qadri, fqadri@icddrb.org, or Jason B. Harris, jbharris@mgh.harvard.edu.

F.Q. and J.B.H. are co-senior authors.

an innate immune response and long-lasting adaptive immunity are not completely understood.

Unlike invasive enteric pathogens, such as *Salmonella enterica* or *Shigella*, *V. cholerae* is noninvasive and does not cause clinically apparent, overt inflammation. Instead, *V. cholerae* colonizes the small intestine and causes secretory diarrhea, mediated by the action of cholera toxin (CT) on intestinal epithelial cells (6). Still, cholera is associated with microscopic inflammatory changes of the human small intestine, which include the widening of intercellular spaces, apical junction abnormalities, vascular congestion, and an influx of neutrophils, mast cells, eosinophils, macrophages, and activated dendritic cells (7–9). In addition, a number of mucosal innate effector molecules, including bactericidal proteins, defensins, lactoferrin, myeloperoxidase, and BPIFB1 (LPLUNC1) are expressed in response to *V. cholerae* infection (10–12).

A previous study of human duodenal RNA expression in cholera, using a microarray-based method, demonstrated that the majority of genes upregulated during acute illness were involved in the innate immune response (10). A subsequent proteomic analysis of the human duodenal mucosa response to cholera demonstrated the upregulation of key innate immune signaling pathways, including activation of the nuclear factor kappa B (NF-κB), the NLRP3 inflammasome, and mitogen-activated protein kinase (MAPK) signaling pathways (13). In addition, a genomic analysis found an association between genetic variants under selection pressure in the NF-κB and inflammasome signaling pathways and susceptibility to cholera (14). Some of these findings can be modeled *in vitro* using cells stimulated by coculture with toxin-producing *V. cholerae*, which results in inflammatory responses mediated by activation of the NF-κB, MAPK, NLRP3, and STAT3 signaling pathways (15–17). Taken together, these studies demonstrate a role for proinflammatory signaling pathways in the innate immune response to cholera. However, previous studies represent only a partial view of the mechanisms of innate immune activation in response to cholera.

To better understand the human innate immune response to cholera, we performed the first transcriptome sequencing (RNA-seq)-based measure of the mucosal transcriptome in patients recovering from acute cholera. RNA-seq provides a higher resolution and a less biased measure of RNA expression than the previously used array-based method. In addition, unlike previous studies, we evaluated the transcriptional response at an additional late time point, comparing the transcriptional response in duodenal tissue during acute cholera with that at subsequent time points, at both 30 and 180 days after infection. Our results confirmed that there is an increase in expression of central innate immune signaling pathways and effectors in acute cholera. Novel findings included the identification of several previously unknown features of the innate immune response to cholera, including the persistence of innate immune activation at 30 days following cholera. As such, this study extends our understanding of the human immune response to this globally important pathogen.

RESULTS

Patient and specimen characteristics. We obtained paired duodenal biopsy specimens from 11 participants during acute cholera (day 2) and subsequently at day 30. We obtained an additional biopsy specimen at day 180 for six of the participants. The characteristics of the participants are listed in Table 1. Ten of the 11 participants were male, and the median age was 30 years. All the participants presented to the International Centre for Diarrheal Disease Research, Bangladesh (ICDDR,B), Hospital in Dhaka, Bangladesh, within 24 h of developing watery diarrhea and had severe dehydration upon presentation; on admission, cultures of stool specimens from all patients were positive for *V. cholerae* O1 of the serotype shown in Table 1. As we have previously observed, most participants demonstrated a significant increase in the vibriocidal antibody titer, though one individual did not develop an antibody response (18). Biopsy specimens had a mean weight of 94 mg (range, 44 to 190 mg). RNA integrity numbers (RIN) ranged from 5.8 to 8.8 (median 7.35). The sequencing depth ranged from 4.0

TABLE 1 Patient characteristics

Patient no.	Age (yr)	Sex	Blood group	*V. cholerae* O1 serotype	Vibriocidal antibody titer on:	
					Day 2	Day 7
1[a]	36	Male	B+	Ogawa	5	5
2[a]	23	Male	O+	Ogawa	160	320
3[a]	30	Male	O+	Inaba	10	40
4[a]	31	Male	B+	Ogawa	160	1,280
5	36	Male	A+	Ogawa	10	640
6[a]	28	Male	A+	Ogawa	5	320
7	38	Male	O+	Ogawa	20	640
8[a]	27	Male	A+	Ogawa	40	1,280
9	36	Male	B+	Inaba	5	2,560
10	28	Male	O+	Ogawa	40	320
11	24	Female	O+	Ogawa	20	640

[a]Participants included in the day 2, 30, and 180 comparisons.

million reads to 108.6 million reads per sample (median, 31.3 million reads per sample) (see Table S1 in the supplemental material).

Transcriptomic profiling reveals upregulation of genes encoding innate immune effectors and signaling molecules. There were 25,269 transcripts detected in the duodenal mucosa in the cholera patients. A paired analysis comparing acute-phase samples (day 2) and convalescent-phase samples (day 30) revealed heterogeneity in the gene expression profiles between participants. Hierarchical clustering analysis identified at least two distinct clusters of participants on the basis of their differential gene expression patterns (Fig. 1). Despite this variation among individual participants, there were still 37 differentially expressed genes for which the difference in expression reached statistical significance across the cohort after correction for multiple comparisons.

These differentially expressed genes included 17 whose expression increased and 20 whose expression decreased during acute cholera (Table 2). Of the 17 genes with increased expression during cholera, 13 are known to be involved in the innate immune response on the basis of the Gene Ontology database. These genes encode signaling molecules involved in lymphocyte and neutrophil recruitment and activation (*CXCL5* and *CXCL9*). Other differentially expressed genes encode the innate effector molecules transcobalamin 1 (*TCN1*), complement factor B (*CFB*), lipocalin 2 (*LCN2*), and dual oxidase 2 (*DUOX2*). Other genes with increased expression in acute cholera are involved in the sensing of microbes and danger signals that lead to the activation of innate signaling pathways. These included the gene encoding Toll-like receptor 8 (*TLR8*), an endosomal Toll-like receptor (TLR) involved in sensing nucleic acids, and the gene encoding guanylate binding protein 5 (*GBP5*), a regulator of the NLRP3 inflammasome. Genes whose expression was decreased during acute cholera were diverse and included those involved in retinol biosynthesis (*LRAT*), gluconeogenesis (*PCK1*), cell proliferation and growth (*TM4SF4*), peptide digestion (*ANPEP*), and ketogenesis (*HMGCS2*); a gene encoding an IgG Fc-binding protein that is abundant in mucus and structurally related to mucin proteins (*FCGBP*); and genes involved in lipid metabolism (*APOC3*, *APOA4*). The differential regulation of a subset of these genes was confirmed using quantitative reverse transcription-PCR (Table S2).

Among the six participants from whom an additional biopsy specimen was obtained at day 180, we found that the number of genes with significantly different levels of expression between day 2 and day 180 (5,431 genes; $n = 6$) was much larger than the number that was apparent in the comparison of the day 2 and day 30 time points (37 genes, $n = 11$). This was not explained simply by the subset of participants for whom data were available at day 180, because data from the six participants evaluated in the day 180 subset revealed only one gene for which the difference in expression reached statistical significance in the day 2 and day 30 comparison (*CFB*; $P = 0.00005$). Instead, the larger number of genes for which the difference in expression reached statistical

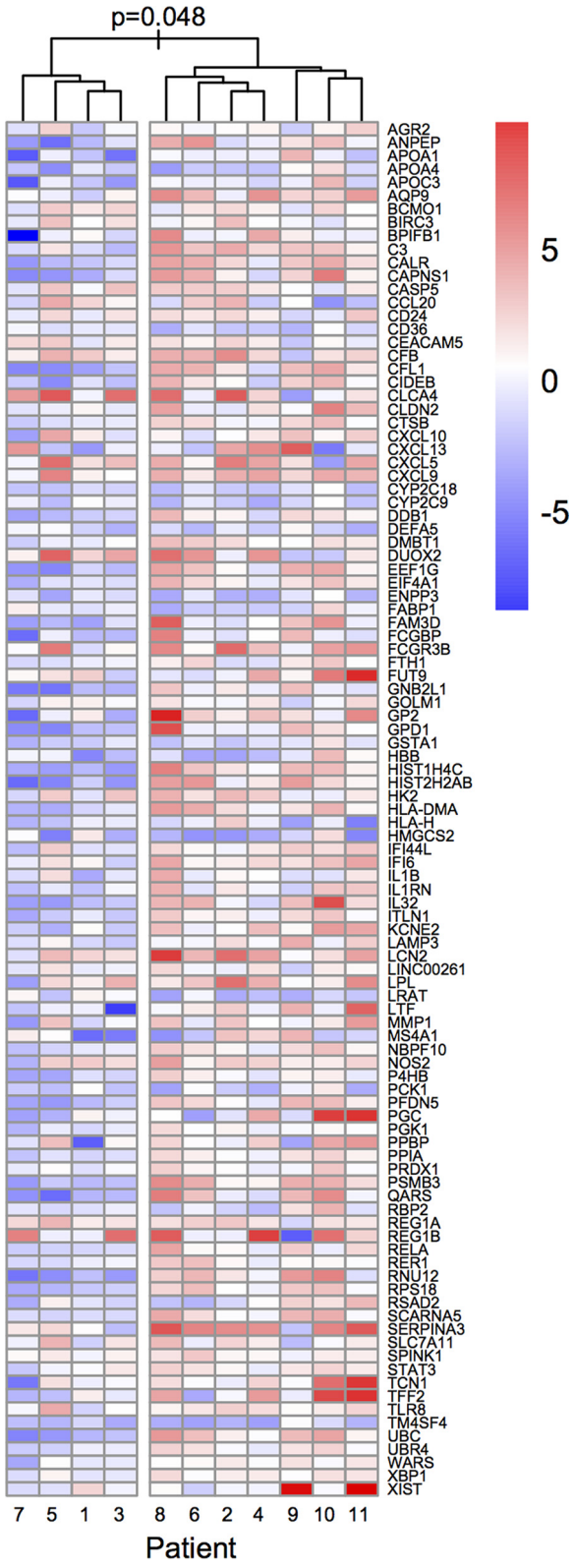

FIG 1 Heatmap representation of 103 genes in the duodenal mucosa of each of the study participants differentially expressed when comparing the acute stage (day 2) to the convalescent stage (day 30) of cholera. The genes are clustered on the basis of the similarity of the gene expression levels. The genes included in this figure were differentially expressed ($P < 0.05$, FDR < 0.05) in at least 3 study participants. A multiscale bootstrap resampling analysis was used for assessing hierarchical clustering, which revealed that patients 1, 3, 5, and 7 formed a cluster which was statistically significant ($P = 0.048$). The numbers at the bottom refer to the individual study participants.

TABLE 2 Genes differentially expressed between days 2 and 30 following cholera

Change in gene expression and gene	Gene product	Log_2 fold change in expression	*P* value[a]
Increased expression on day 2			
XIST	Long noncoding RNA	7.35	0.0001
CXCL9	CXC chemokine 3 (lymphocyte chemoattractant)	1.96	0.00005
FCGR3A	Receptor for Fc portion of IgG expressed on NK cells	1.95	0.00005
SERPINA3	Member of the serine protease inhibitor class	1.94	0.00005
CXCL5	CXC chemokine 5 (neutrophil activation and recruitment)	1.94	0.00005
LCN2	Lipocalin 2 (iron trafficking protein)	1.8	0.00005
CFB	Complement factor B	1.78	0.00005
DUOX2	Dual oxidase 2	1.57	0.00005
REG1A	Regenerating islet-derived protein 1A	1.38	0.00005
TCN1	Transcobalamin I (vitamin B_{-12} binding protein)	1.32	0.0001
TLR8	Toll-like receptor 8	1.22	0.00005
ITM2C	Integral membrane protein 2C	1.13	0.00005
BCMO1	Beta-carotene oxygenase 1	1.04	0.00015
SLC7A11	Solute carrier family 7 member 11	0.985	0.00015
GBP5	Guanylate binding protein 5	0.934	0.00015
CEACAM5	Carcinoembryonic antigen-related cell adhesion molecule 5	0.915	0.0001
SPINK1	Serine peptidase inhibitor, Kazal type 1	0.901	0.00005
Decreased expression on day 2			
APOC3	Apolipoprotein C3	−2.99	0.00005
RNU12	Long noncoding RNA	−2.34	0.00005
FCGBP	Fc fragment of IgG binding protein	−2.19	0.00015
TM4SF4	Intestine and liver tetraspan membrane protein	−1.7	0.00005
HBB	Beta hemoglobin	−1.61	0.00005
CFL1	Colfilin-1 protein	−1.58	0.00005
HMGCS2	3-Hydroxy-3-methylglutaryl coenzyme A synthase 2	−1.55	0.00005
ANPEP	Alanyl aminopeptidase	−1.46	0.00005
UBC	Ubiquitin C	−1.29	0.00005
APOA4	Apolipoprotein A4	−1.18	0.00005
HIST1H4C	Histone cluster 1, H4c	−1.15	0.0001
PCK1	Phosphoenolpyruvate carboxykinase 1	−1.13	0.00005
UGT2B7	UDP-glucuronosyltransferase 2B9	−1.12	0.00005
LRAT	Lecithin retinol acyltransferase	−1.09	0.00005
CYP2C18	Cytochrome P450, family 2, subfamily C, polypeptide 18	−1.08	0.00005
EEF1G	Eukaryotic translation elongation factor 1 gamma	−1.07	0.00005
CTSE	Cathepsin E	−0.98	0.00005
ADH4	Alcohol dehydrogenase 4	−0.95	0.0001
CYP2C9	Cytochrome P450, family 2, subfamily C, polypeptide 9	−0.91	0.0001
GSTA1	Glutathione *S*-transferase alpha 1	−0.87	0.00005

[a]*P* values adjusted for multiple comparisons with a false discovery rate of <0.05.

significance was due to a robust difference in mucosal gene expression among a larger number of transcripts when expression during acute cholera (day 2) was compared with that at day 180. The majority of these differentially regulated genes (3,369 of 5,431, or 62%) demonstrated increased expression on day 2 relative to that on day 180 (Fig. 2).

To explore this time course further, we considered the top 100 genes most differentially expressed between acute cholera and day 180 on the basis of statistical significance. Clustering analysis on the basis of their expression at the three time points revealed at least four distinct patterns for the time course of gene expression (Fig. 3). The majority of the genes (clusters A, B, and C) demonstrated their highest levels of expression at day 2 and their lowest levels of expression at day 180. These three clusters could be distinguished by their level of expression at day 30. The levels of expression of some genes remained increased in at day 30 (cluster A, persistently increased), other genes had intermediate levels of expression at day 30 (cluster B), and the expression of some genes returned quickly to lower levels (cluster C, transiently increased). A smaller set of genes (cluster D) demonstrated their peak level of increased expression at day 30. Overall, these findings reveal persistent gene expression changes up to 30 days after infection with *V. cholerae*, a novel finding not previously described in cholera.

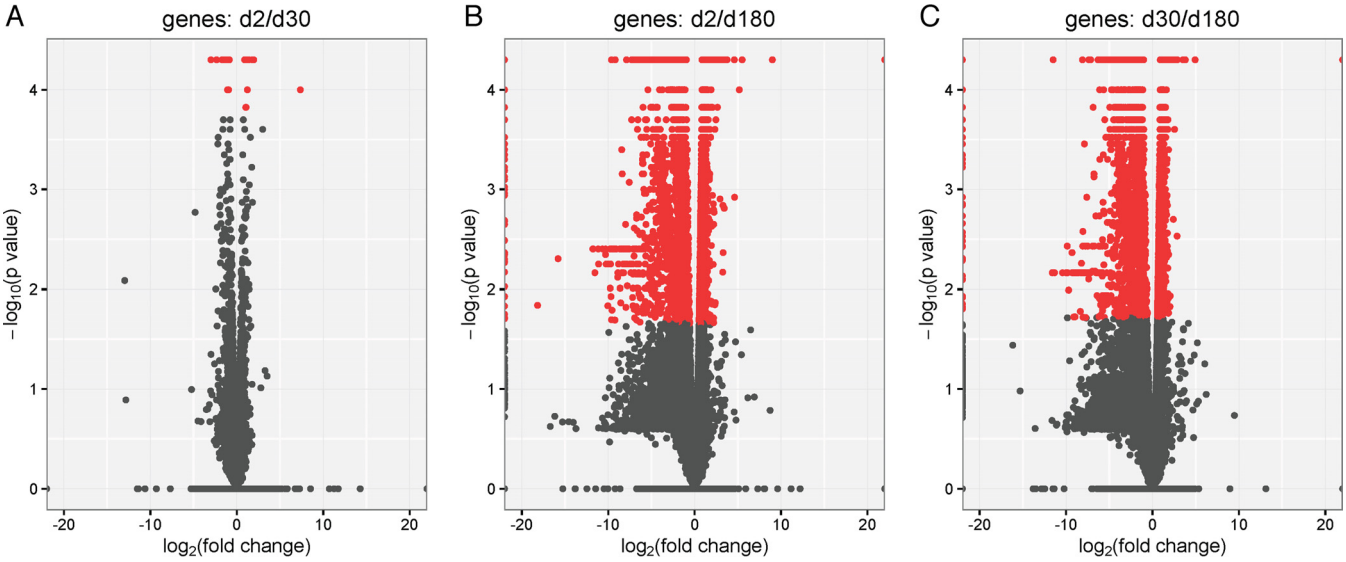

FIG 2 Volcano plot of RNA-seq data demonstrating differentially expressed genes in acute-phase (day 2 [d2]) versus convalescent-phase (day 30 [d30]) samples (A), acute-phase (day 2) versus day 180 (d180) samples (B), and day 30 versus day 180 samples (C). The *y* axis values show the negative logarithm base 10 of the *P* value. The *x* axis is shown as the $\log_2$ difference in estimated relative expression values. The red dots represent reads with a statistically significant difference in expression, defined as a *P* value of <0.05 and an FDR of <0.05.

As expected, the set of genes that had transiently increased expression (cluster C) overlapped the set of genes that were differentially expressed between days 2 and 30 in the data from the full cohort. Of the 17 genes whose expression was significantly increased when the expression for specimens collected on days 2 and 30 was compared, 11 were in cluster C. Other genes in this category whose expression was transiently increased included those for caspase-1 (*CASP1*), caspase-5 (*CASP5*; a regulator of the NLRP3 inflammasome), and hexokinase 2 (*HK2*; a cytoplasmic sensor of peptidoglycan and a regulator of the NLRP3 inflammasome).

Use of the InnateDB database to evaluate the ontogeny of genes differentially regulated between acute cholera and day 180 revealed that 286 of the genes upregulated during the acute phase of cholera were involved in the innate immune response, 149 genes were involved in apoptosis, 62 genes were involved in the cellular response to DNA damage stimulus, 41 genes were involved in Toll-like receptor signaling, and 18 genes were involved in NF-κB signaling. Furthermore, there was a broad upregulation of TLRs, including TLRs 1 to 8 and 10. Of the genes found to be downregulated when expression on day 2 was compared to that on day 180, 198 genes were involved in metabolic processes, 180 genes were involved in the innate immune response, and 89 genes were involved in the apoptotic process (Table S3) (19).

Innate immune pathways and central innate immune signaling molecules activated by *V. cholerae*. We used Ingenuity Pathway Analysis (IPA) to identify biological pathways enriched by *V. cholerae* infection and predict the upstream transcriptional regulators activated in the duodenal mucosa in response to cholera (Fig. 4A and B). Using this approach, central innate immune pathways identified to be activated during the acute phase of cholera included the NF-κB signaling, MAPK signaling, TREM1 signaling, and stress-activated protein kinase (SAPK)/Jun N-terminal protein kinase (JNK) signaling pathways. Toll-like receptor signaling was also enriched, as our data demonstrated an upregulation of multiple Toll-like receptors, including cell surface TLRs 1, 2, 4, 5, and 6, as well as the endosomal TLRs, including TLR3, TLR7, and TLR8. In addition, there was increased expression of TLR10 during the acute phase of cholera. Our analysis also revealed an enrichment of expression of genes involved in the production of nitric oxide and reactive oxygen species.

We also used IPA to predict which cytokines and transcription factors may be activated during cholera (Table 3). The top upstream cytokines predicted to be acti-

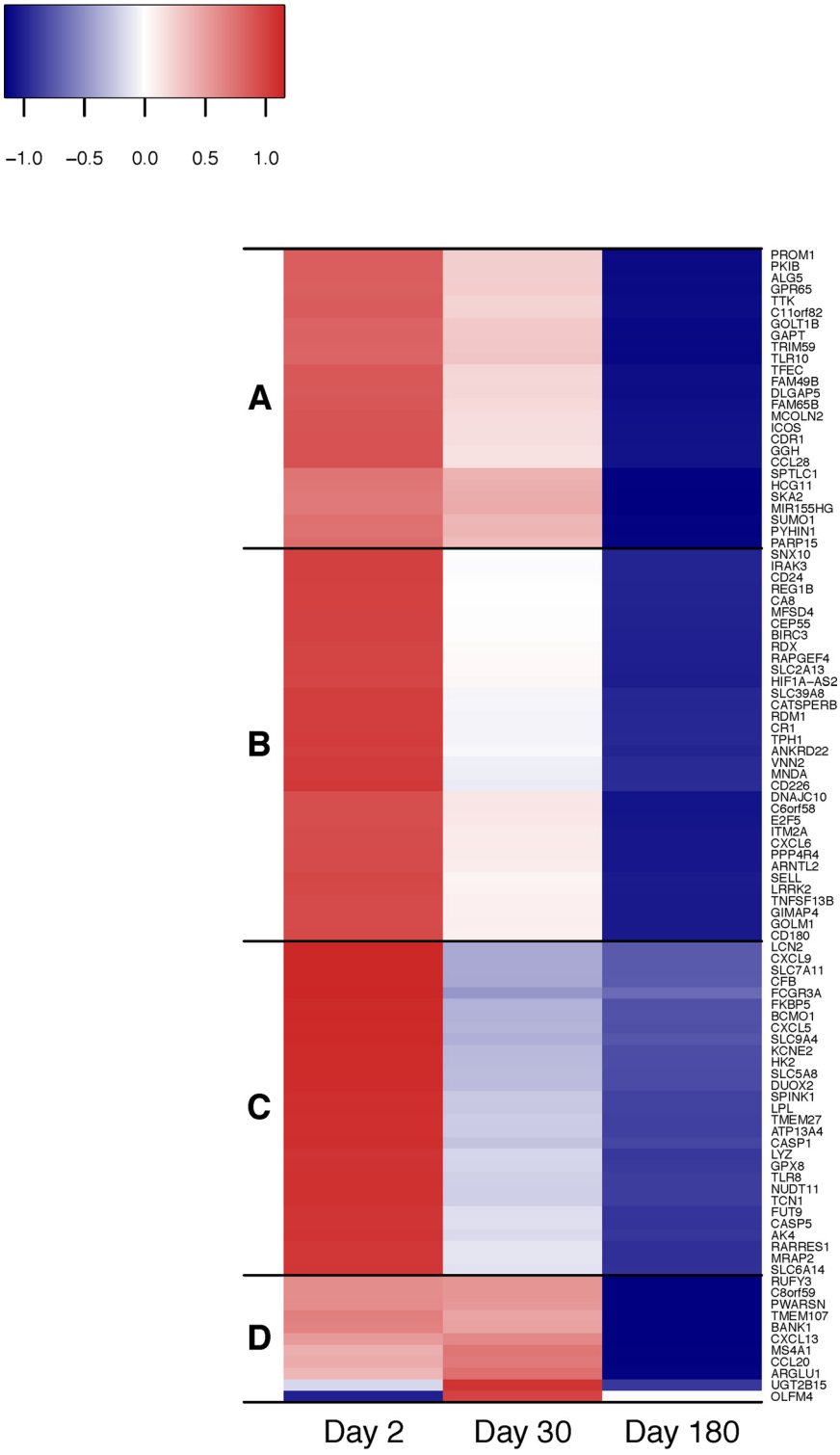

FIG 3 Heatmap representing the gene expression values (FPKM) of the top differentially expressed genes across the 3 time points: days 2, 30, and 180. The genes in cluster A demonstrated persistently increased expression at day 30. The genes in cluster B demonstrated increased expression at day 2 and intermediate levels of expression at day 30. The genes in cluster C demonstrated a transient increase in expression at day 2 and lower levels of expression at days 30 and 180. The genes in cluster D had increased expression at day 30 compared to that at day 2 and day 180.

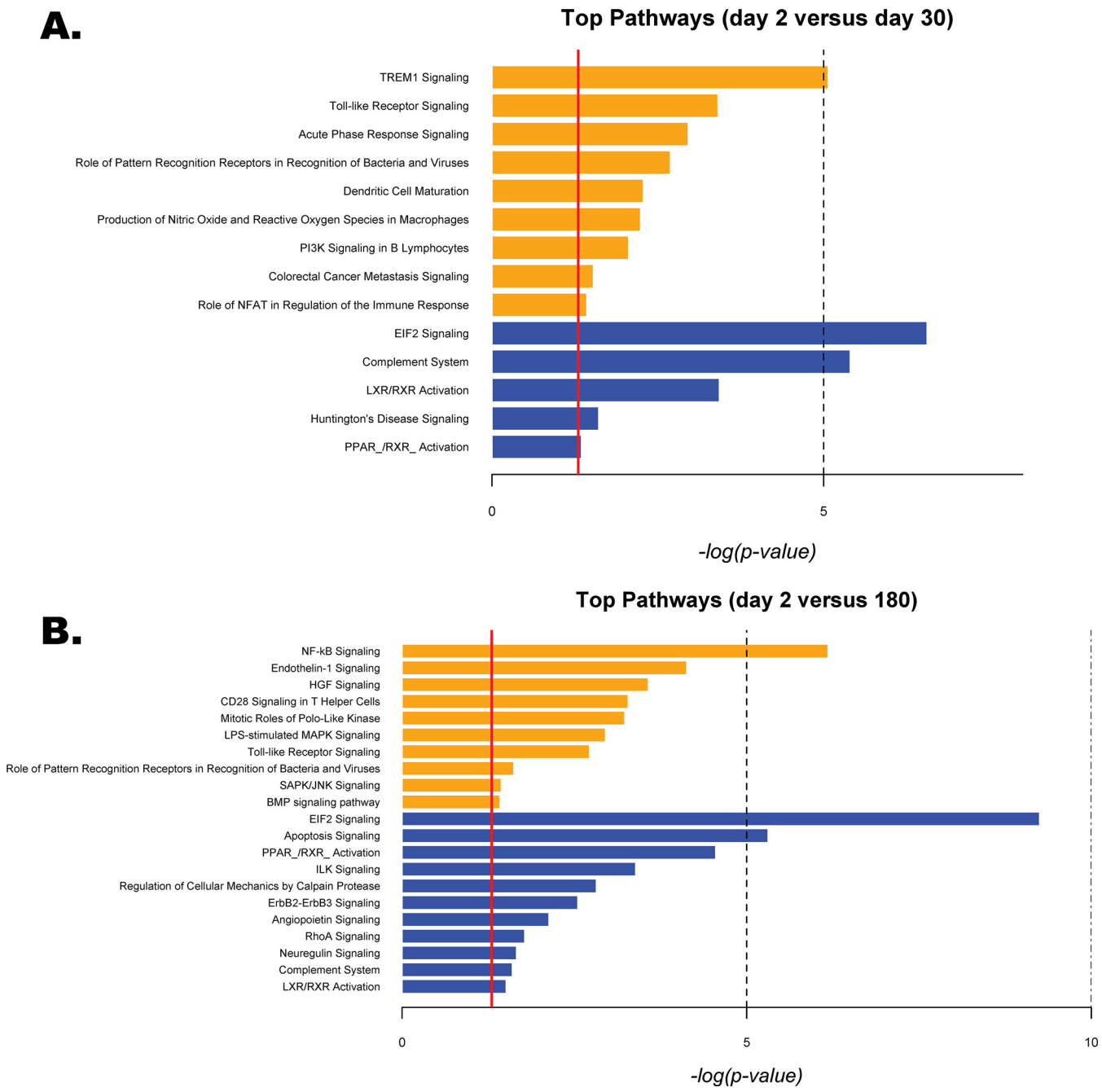

FIG 4 Canonical pathways predicted by IPA to be activated or inhibited in the duodenal mucosa of patients with cholera, comparing the results for expression on days 2 and 30 (A) or days 2 and 180 (B). Pathways predicted to be activated are in orange, and the blue bars correspond to pathways predicted to be inhibited (based on the Z-scores determined by IPA). The red line denotes the threshold of statistical significance [$P < 0.05$ or $-\log(P \text{ value}) = 1.3$]. PI3K, phosphatidylinositol 3-kinase; NFAT, nuclear factor of activated T cells; EIF2, eukaryotic initiation factor 2; LXR, liver X receptor; RXR, retinoid X receptor; PPAR, peroxisome proliferator-activated receptor; HGF, hepatocyte growth factor; ILK, integrin-linked kinase.

vated during cholera were gamma interferon, alpha 2 interferon, beta 1 interferon, interleukin-1β (IL-1β), IL-6, oncostatin-M (OSM), colony-stimulating factor 2 (CSF2), IL-21, and IL-23. The top upstream transcriptional regulators predicted to be activated during acute cholera were interferon regulatory factor 7 (IRF7) and STAT1.

Immunostaining for DUOX2 and TLR8 demonstrates expression in the duodenal mucosa. One of the genes with the most robustly increased expression during acute cholera, *DUOX2*, encodes an oxidase that produces bactericidal reactive oxygen species and is an effector of the inflammasome-mediated antibacterial response (20).

TABLE 3 Top upstream regulators predicted by IPA to be activated during cholera[a]

		Days 2 to 30		Days 2 to 180	
Upstream regulator	Type	Z-score	*P* value	Z-score	*P* value
Oncostatin-M (OSM)	Cytokine	3.299	1.61E−11	3.657	1.10E−09
IRF7	Transcription regulator	3.236	9.77E−05	2.795	1.88E−03
IL-1β	Cytokine	3.217	4.61E−16	3.961	2.00E−09
Gamma interferon	Cytokine	3.087	2.94E−24	2.936	4.44E−13
IL-6	Cytokine	2.955	3.92E−16	NS	NS
STAT1	Transcription regulator	2.945	9.32E−14	NS	NS
Beta 1 interferon	Cytokine	2.786	6.51E−07	NS	NS
CSF2	Cytokine	2.602	1.22E−10	3.656	7.54E−13
Tumor necrosis factor	Cytokine	2.599	7.34E−16	NS	NS
Alpha 2 interferon	Cytokine	2.570	2.18E−05	NS	NS
REL	Transcription regulator	NS	NS	2.739	1.77E−02
IL-21	Cytokine	NS	NS	2.733	7.64E−03
IL-23	Cytokine	NS	NS	2.611	1.91E−02

[a]Default IPA settings were used to generate the list, which was then restricted to include cytokines and transcriptional regulators only. NS, nonsignificant.

We examined the expression of DUOX2 in the human duodenal mucosa in acute- and convalescent-phase cholera using immunohistochemistry (IHC). The robust expression of DUOX2 was seen in the epithelial cells of the duodenal surface during the acute phase of cholera. Sections obtained at the acute and convalescent (day 30) phases clearly differed in their immunostaining for DUOX2 (Fig. 5). Quantification of the expression of DUOX2 in the duodenal tissue sections showed a statistically significant increase in expression ($n = 3$ subjects at each time point, with three sections per subject per time point; mean, 8,152 cells/mm^2 in day 2 specimens versus 4,237 cells/mm^2 in day 30 specimens; $P = 0.0310$).

TLR8 expression was also increased during acute cholera. However, the role of TLR8 in cholera pathogenesis is unknown, and we sought to further define its expression in the duodenal mucosa of cholera patients. TLR8 is expressed in intracellular vesicular membranes of monocytes, macrophages, and myeloid dendritic cells (21). Using IHC, we examined the expression of TLR8 in acute-phase (day 2) duodenal tissue sections and compared this to that in convalescent-phase (day 30) specimens. TLR8 expression was predominantly seen in the lamina propria of the duodenal mucosa during the acute phase of cholera and not in epithelial cells (Fig. 6). There was a trend toward increased expression of TLR8 in the acute-phase specimens ($P = 0.07$; mean, 2,685 cells/mm^2 in day 2 specimens versus 1,513 cells/mm^2 in day 30 specimens).

***In vitro* models also demonstrate increased expression of *DUOX2* and *TLR8* in response to stimulation with live *V. cholerae* O1.** Using polarized Caco-2 epithelial cells, the expression of *DUOX2* was increased following stimulation with live, toxin-producing *V. cholerae* O1 relative to that following stimulation with heat-inactivated *V. cholerae* O1, CT, or medium alone (Fig. 7A). Using phorbol myristate acetate (PMA)-stimulated THP-1, macrophage-like cells, we similarly found that *TLR8* gene expression was increased in cells stimulated with live, toxin-producing *V. cholerae* O1 compared with cells stimulated with heat-inactivated *V. cholerae* O1, CT, or medium alone (Fig. 7B).

DISCUSSION

We conducted the first analysis of the human mucosal transcriptional response to *V. cholerae* infection using RNA-seq. Our results demonstrate the increased expression of genes involved in central pathways of the innate immune response during acute cholera. While prior work has shown a prominent role of the innate immune response during acute infection with *V. cholerae*, the present study provides a broader look into the human mucosal transcriptome and reveals novel components of innate immune signaling pathways during the acute phase of cholera (10, 13, 14). Important findings of this study include a persistence of gene expression 30 days after initial infection with *V. cholerae*, activation of components of the innate immune response not previously

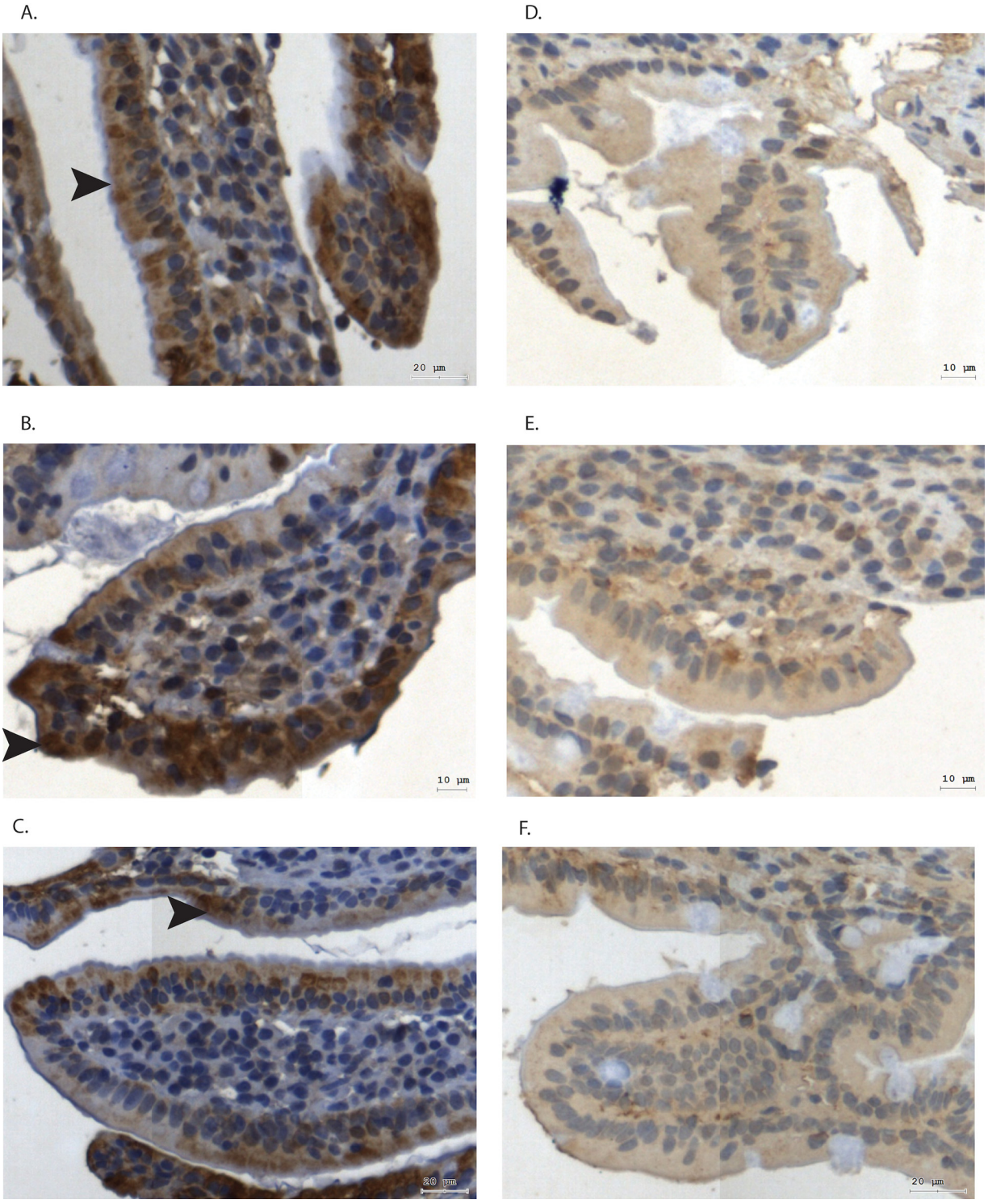

FIG 5 Immunohistochemistry demonstrating the expression of DUOX2 during acute cholera in paraffin-preserved duodenal tissue biopsy specimens. DUOX2 expression localized to the epithelial surface (arrowheads), and expression of DUOX2 in the duodenal mucosa during the acute phase of cholera (A to C) was observed to be increased compared to that during the convalescent phase (D to F) ($n = 3$ subjects at each time point with three sections per subject per time point; mean = 8,152 cells/mm^2 in day 2 specimens versus 4,237 cells/mm^2 in day 30 specimens; $P = 0.0310$). The sections obtained during the acute and convalescent phases shown in the figure were obtained from the same individual. The images were captured using a TissueFAXS slide scanner, which captures many microscopic fields of view (FOV) over large areas of each tissue section with a high-resolution camera and then aligns each FOV to create a large single view (montage) of the entire tissue section. At high magnifications, the boundaries (lines) between adjacent fields of view might be visible due to slight misalignments during the slide scanning process, and these amount to only a few micrometers of overlap of adjacent FOV.

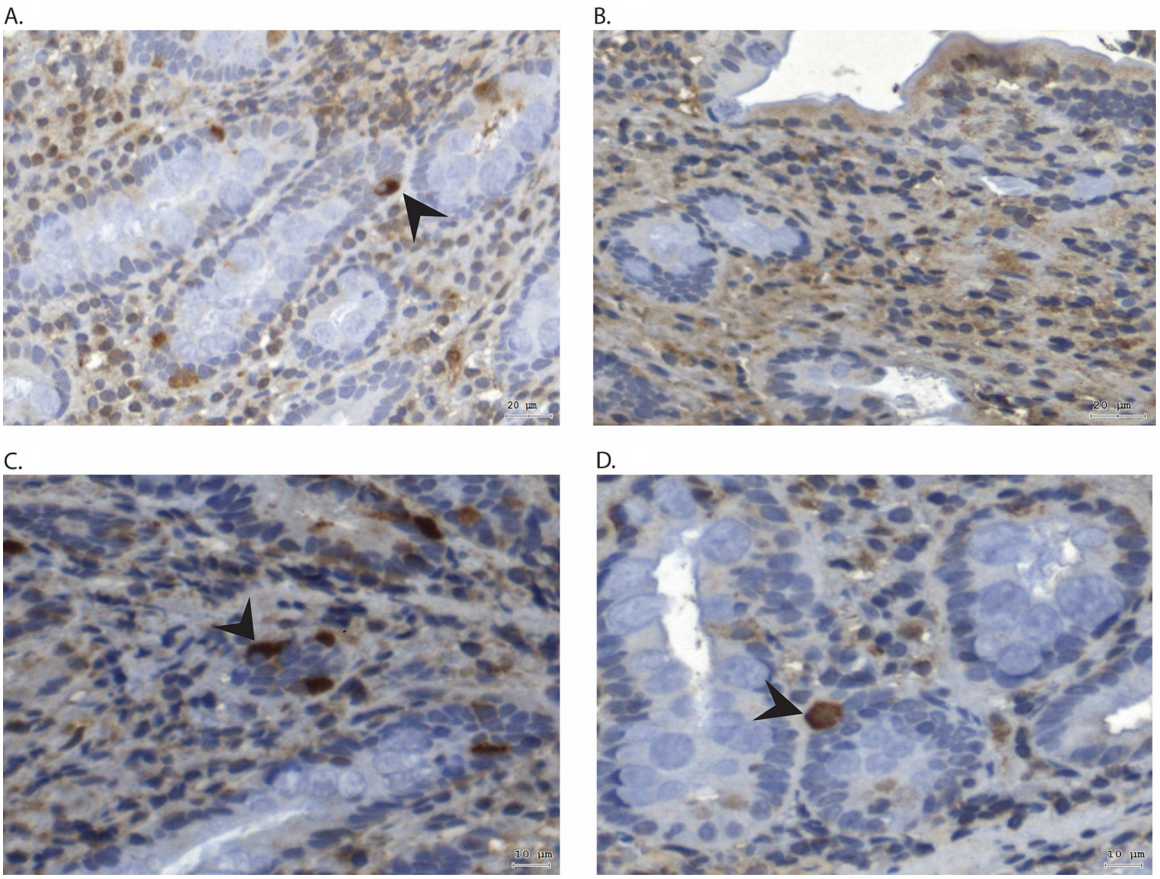

FIG 6 Immunohistochemistry demonstrating TLR8 expression during acute cholera in paraffin-preserved duodenal tissue biopsy specimens. TLR8 expression is observed predominantly in the lamina propria of the duodenal mucosa during acute cholera (A, C, and D), with a trend toward increased expression in the acute phase of cholera compared to that in the convalescent phase (B) ($n = 3$ subjects at each time point with three sections per subject per time point; mean, 2,685 cells/mm^2 in day 2 specimens versus 1,513 cells/mm^2 in day 30 specimens; $P = 0.071$). Arrowheads, examples of strongly positively staining cells. The specimens in this figure include tissue sections from multiple subjects, and given that there was not a robust expression of TLR8, multiple high-power fields of acute-phase specimens were included to adequately demonstrate the TLR8 expression that we observed.

described in the human immune response to *V. cholerae*, and the fact that activation of some of the genes may be dependent on live toxigenic *V. cholerae* rather than heat-inactivated bacteria.

Unexpectedly, the activation of central inflammatory pathways persisted even at 30 days after infection. This suggests that despite the rapid resolution of symptoms in cholera, infection leads to a prolonged disruption of intestinal homeostasis persisting for over a month. As such, our study provides an unexpected demonstration of how a single episode of noninvasive, secretory diarrhea may result in prolonged changes in the mucosal immune system. Considering the epidemiologic association between repeated episodes of secretory diarrhea and the development of chronic enteropathy in childhood, our finding of persistent immune activation following cholera is particularly notable (22). While the consequence of persistent immune activation following infection is unknown, the question of whether this state could be detrimental or perhaps provide protection from reinfection or infection with other enteropathogens warrants further investigation. More generally, our results build on previous studies to shed light on the specific features of the innate immune response to cholera (13). These features of the innate response include the array of pattern recognition receptors, signaling pathways, and innate immune effectors which are expressed or activated in response to infection. Thus, this study identifies a broad range of innate immune signaling pathways activated in the human intestinal mucosa during infection with *V. cholerae*.

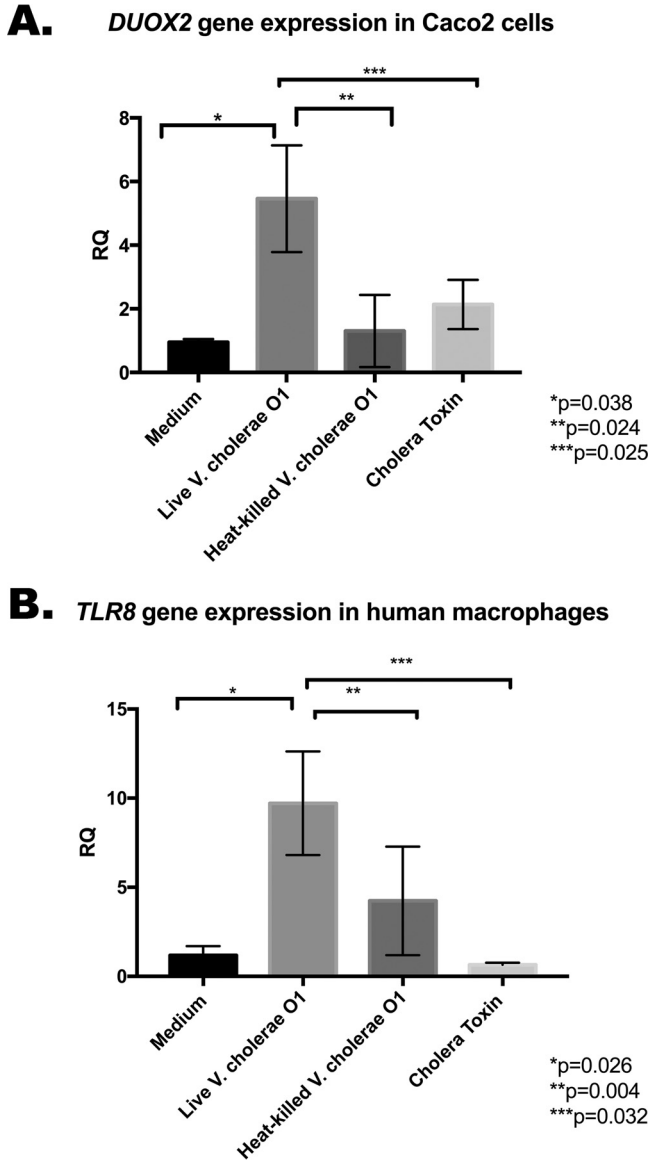

FIG 7 (A) Intestinal epithelial cells (a polarized Caco-2 cell monolayer) stimulated with *V. cholerae* O1 exhibited increased expression of DUOX2 compared to that by cells in medium alone, cells stimulated with heat-inactivated *V. cholerae* O1, and cells stimulated with cholera toxin alone ($P = 0.038$, $P = 0.024$, and $P = 0.025$, respectively). (B) THP-1 cells differentiated to macrophages were stimulated with *V. cholerae* O1, heat-inactivated *V. cholerae* O1, and cholera toxin alone. Macrophages showed increased expression of TLR8 following stimulation with live *V. cholerae* O1 compared to that following stimulation with medium alone, heat-inactivated *V. cholerae* O1, and cholera toxin alone ($P = 0.026$, $P = 0.004$, and $P = 0.032$, respectively).

Together, our findings and those of previous studies indicate that multiple pathogen- and danger signal-sensing mechanisms are likely engaged when live *V. cholerae* O1 interacts with the intestinal mucosa. Previous *in vitro* studies have demonstrated that *V. cholerae* O1 activates multiple cell surface TLR/MyD88 signaling pathways. These signaling events include *V. cholerae* O1 lipopolysaccharide (LPS), which signals via TLR4, and cytolysin (HlyA), which signals via TLR2/TLR6 heterodimers (13, 23, 24). Because *V. cholerae* possesses a sheathed flagellum, it is less clear whether TLR5-mediated signaling contributes to the response (25). In addition, it remains unclear whether lipid A modifications that occur *in vivo* can impact TLR4 signaling (26). However, on the basis of the increased expression of several cell surface TLRs, including TLRs 2, 4, 5, and 6, during acute cholera and a sustained increase in NF-κB pathway

activation following cholera, this study provides further evidence that multiple cell surface TLR/MyD88-dependent signaling pathways may contribute to the sustained activation of NF-κB signaling (6, 25, 27).

Our present study also provides new *in vivo* evidence that endosomal TLRs may play a role in the innate immune response to cholera. This study is the first to demonstrate the coordinated activation of a broad range of cell surface and endosomal TLRs in the setting of *V. cholerae* infection. In particular, we found an increase in the expression of genes for endosomal TLRs, including *TLR3*, *TLR7*, *TLR10*, and *TLR8*. In the setting of cholera, the upregulation of the endosomal TLRs is a novel finding, and *TLR8* exhibited the greatest change in expression between the acute and convalescent phases of cholera. This is notable, because unlike cell surface TLRs, endosomal TLR signaling results in the downstream production of type I interferons through an IRF7-dependent signaling pathway (21). Thus, our finding that IRF7 and beta 1 and alpha 2 interferons were among the top predicted activated upstream regulators suggests the potential relevance of this pathway in the immune response to *V. cholerae* infection.

The potential physiologic relevance of these findings is underscored by our observation that TLR8 expression is increased in differentiated THP-1 cells upon stimulation with toxigenic *V. cholerae* O1. Interestingly, neither heat-inactivated *V. cholerae* O1 nor CT alone resulted in a robust increase in the expression of TLR8. This suggests that the induction of TLR8 expression may depend on bacterial viability. Interestingly, it has recently been shown that bacterial RNA activates TLR8 and that both *Escherichia coli* and the phagocytosis of *Helicobacter pylori* induce TLR8 activation in human cell culture models of infection (28, 29). Thus, the differential expression of TLR8 in response to stimulation with live *V. cholerae* O1 could reflect a requirement for sensing bacterial RNA, which is rapidly lost in heat-killed bacteria (30). Considering these results together, our findings suggest that increased TLR8 expression during acute cholera may provide an important endosomal TLR signaling pathway that is specific to live bacteria and relevant to the activation of the IRF7/type I interferon response that appears to be a hub of the innate immune response in human cholera.

In addition to TLR-mediated pathogen sensing and activation of the NF-κB and IRF7 transcription factors, our study suggests that the NLRP3 inflammasome is another major hub of the innate immune response to cholera. Previously, we and others have demonstrated that CT leads to activation of the NLRP3 inflammasome in LPS-primed murine macrophages and that this activation is dependent on noncanonical activation by caspase-11 (14, 31). In this study, we found that both the gene for caspase-5 (one of two human orthologs of murine caspase-11) and *GBP5* (a regulator of the NLRP3 inflammasome assembly that responds to soluble bacterial cell wall components [32]) were increased in expression during acute cholera. This finding is consistent with the findings of previous studies by our group demonstrating that IL-1β production is increased in lamina propria lymphocytes during acute cholera and with the findings of the current IPA analysis that predicts that IL-1β is one of the top upstream regulators activated during acute cholera.

In addition to these findings, we observed novel aspects of the effector arm of the innate mucosal antibacterial response following cholera. In particular, the robust activation of *DUOX2* highlights a potential role of reactive oxygen species and oxidative stress in the pathogenesis of cholera. While it has not previously been shown to play a role during cholera specifically, DUOX2 impacts the maintenance of intestinal homeostasis, and its aberrant expression has been linked to inflammatory bowel disease (33). Germfree mice receiving a dysbiotic microbiota but not those receiving a healthy microbiota exhibited increased expression of DUOX2, suggesting that it is an important modulator of the host-microbiota interaction (34). Thus, the robust but transient upregulation of *DUOX2* following infection with *V. cholerae*, which we confirmed both in Caco-2 cells *in vitro* and in epithelial cells in immunohistochemical analysis, may modulate the changes in the microbiome induced by cholera (35).

Some limitations of this study also merit consideration. Our study cohort included only 11 participants and 6 subjects from whom a biopsy specimen was obtained at 180

days after infection. These participants demonstrated heterogeneous gene expression profiles. Nevertheless, we were still able to identify significant changes in gene expression across the cohort, and our results were consistent with those of previous studies of the immune response in the duodenal mucosa of patients infected with *V. cholerae* O1 performed using other methods (10, 13). One limitation of this study is the lack of uninfected, matched controls, as we were unable to obtain specimens from such individuals. However, the longitudinal design of this study, with samples being obtained 180 days after infection, serves as a control to assess the acute changes in transcription due to *V. cholerae* infection. In addition, the *in vitro* models serve to further support key observations in these participants. Another limitation of our study is that the participants received medical therapy, including antibiotics and fluid resuscitation, which may have confounded the changes in gene expression at the mucosal surface. Additionally, the subjects in this study reside in a region where there is an elevated incidence of enteric infections, including infections caused by pathogens other than *V. cholerae*, and coinfection may serve as a potential confounder. However, cultures of stool specimens were performed for each individual to evaluate them for other enteric pathogens, and if such pathogens were identified, they were excluded from the study. Finally, while samples were taken from the duodenum, colonization by *V. cholerae* also occurs at more distal sites in the small intestine (36).

Despite these limitations, our investigation provides a novel vantage point from which to evaluate the innate immune response to *V. cholerae* infection in its natural human host. We found that cholera induces a robust inflammatory response in the intestinal mucosa, with gene expression changes persisting for at least 30 days after infection. Our results suggest potential novel mechanisms for the activation of several central pathways of the mucosal innate immune response, notably, those involved in pathogen sensing via both endosomal TLR signaling and regulation of the NLRP3 inflammasome. Further study is needed to determine which of these early responses to *V. cholerae* O1 are critical for successful pathogen eradication in the short term as well as the subsequent generation of long-term adaptive immunity that follows cholera.

MATERIALS AND METHODS

Participant enrollment and collection of duodenal biopsy specimens. Adults presenting to the International Centre for Diarrheal Disease Research, Bangladesh (ICDDR, B), in Dhaka, Bangladesh, with severe acute watery diarrhea due to *V. cholerae* O1 infection were recruited for this study. Those who agreed to participate underwent a screening history and physical examination, including laboratory testing. All adults with culture-confirmed cholera due to *V. cholerae* O1 infection, no other underlying conditions, and no evidence of coinfection with another enteric pathogen were eligible for the study. For each individual, stool studies were done to assess the subject for infections with other enteropathogens, and if any such enteropathogens were identified, the subject was excluded from the study. All participants received antibiotics and intravenous fluids as part of the standard of care for cholera. Once the participants were fully rehydrated (within 24 h of presentation), we collected six duodenal pinch biopsy specimens from the second part of the duodenum by esophagogastroduodenoscopy (EGD). We then collected convalescent-phase biopsy specimens 30 and 180 days later from the same subjects. Tissue was stored in RNAlater solution (Qiagen, Hilden, Germany) at −80°C, and one biopsy specimen from each time point was preserved in paraffin. The ICDDR,B Ethical and Research Review Committees and Massachusetts General Hospital's Institutional Review Board approved the study.

Sample preparation, RNA sequencing, and differential expression analysis. We homogenized the biopsy specimens in TRIzol reagent (Life Technologies, Carlsbad, CA, USA) and performed RNA extractions according to the manufacturer's recommendations (37). We removed rRNA with an Illumina Ribo-Zero rRNA removal kit (Illumina, Inc. San Diego, CA, USA) and confirmed the RNA quality using an Agilent bioanalyzer (Agilent Technologies Inc., Palo Alto, CA, USA). We constructed cDNA libraries using a PrepX RNA-seq for Illumina Library kit. We sequenced these libraries as 100-bp single-end reads on an Illumina HiSeq 2500 instrument.

Differential expression and pathway analysis. We aligned the sequencing reads to the sequence of a human reference genome, UCSC Hg19, using the TopHat2 program, annotating exons and calculating the values of the number of fragments per kilobase per million (FPKM). We analyzed differential gene expression with the Cufflinks/Cuffdiff program, comparing the transcriptome during acute cholera with that in samples collected on day 30 and day 180 (38, 39). We considered genes to be differentially expressed when the $\log_2$ fold change met the threshold for significance with a P value of <0.05 adjusted for a false discovery rate (FDR) of <0.05 and using the Benjamini-Hochberg correction for multiple testing. We confirmed the differential expression of selected genes using real-time quantitative PCR with SYBR green. We used a hierarchical clustering analysis to identify distinct clusters of subjects based on their gene expression profiles. We evaluated for pathway enrichment and the activity

of upstream regulators using Qiagen Ingenuity Pathway Analysis (IPA; Qiagen, Redwood City, CA) commercial software (40). For this analysis, we used gene expression data sets comparing day 2 versus day 30 specimens and day 2 versus day 180 specimens as input for IPA with the $\log_2$ fold change and adjusted *P* values (using FDR cutoffs of 0.05 and 0.01 for the respective analyses). We implemented the IPA analysis using the software manufacturer's default settings.

Immunostaining and image analysis. We performed immunohistochemistry (IHC) to screen for DUOX2 and TLR8 expression using 5-μm paraffin-preserved sections. A total of three tissue sections from three different patients from both the day 2 and day 30 time points were included. Slides were deparaffinized, blocked with dual endogenous enzyme block (DEEB) 5′ (Dako Agilent, Santa Clara, CA, USA), and then incubated with either polyclonal anti-DUOX2 antibody (Thermo Fisher, Rockford, IL, USA) or polyclonal anti-TLR8 antibody (Pro-Sci, Poway, CA, USA) at a 1:250 dilution. The slides were incubated with a secondary antibody, a horseradish peroxidase-conjugated anti-rabbit immunoglobulin polymer with hematoxylin as a counterstain. We obtained high-resolution images using a TissueFAXS slide-scanning platform, quantified the staining using HistoQuest software (TissueGnostics, Vienna, Austria), and included a measure of nuclear staining to allow reliable cell counting. We quantified the mean intensity of each marker and enumerated positively staining cells to calculate the number of target protein-expressing cells per square millimeter for each section of tissue. We then determined the significance of the differences between acute-phase (day 2) and convalescent-phase (day 30) samples using a paired *t* test.

The images were generated using a TissueFAXS slide scanner (TissueGnostics USA), which captures microscopic fields of view (FOV) of the tissue section in the *x-y* plane using a Zeiss Axio Imager Z2 microscope with a motorized stage and high-resolution camera (Baumer HXG40c HX series CMOS 16-bit color camera). These FOV are then stitched together to create a single large image (or montage) of the entire tissue region for cell identification and quantification. The stitching process involves alignment of a certain amount of overlap of each FOV image and must be carefully calibrated for a given microscope objective and camera.

***In vitro* cell culture stimulation assays.** We cultured human monocytic THP-1 cells in RPMI with 20% heat-inactivated fetal bovine serum (FBS) and 1% Gibco antibiotic-antimycotic mixture (10,000 units/ml of penicillin, 10,000 μg/ml of streptomycin, 25 μg/ml of amphotericin B) at 37°C in 5% CO_2. We then seeded 24-well culture plates with 5×10^5 cells/ml, added phorbol myristate acetate (PMA) at a concentration of 10 ng/ml, and incubated the plates for 48 h to allow the cells to differentiate into human macrophage-like cells. We also cultured human intestinal epithelial Caco-2 cells in Dulbecco's modified Eagle's medium (DMEM) with FBS and the antibiotic-antimycotic mixture described above. We seeded the Caco-2 cells at 1×10^6 cells/ml and incubated them at 37°C in 5% CO_2 for 15 days to allow the formation of a polarized epithelial cell monolayer. To stimulate the cells, we grew live *V. cholerae* O1 bacteria (reference strain N16961) under ToxR-inducing conditions as described previously (41). The bacterial cultures were then centrifuged and suspended in medium. We stimulated the THP-1 or Caco-2 cells with 100 μl of live *V. cholerae* O1, 100 μl of heat-inactivated *V. cholerae* O1 (1.5×10^8 CFU/ml), or purified CT (List Biological Laboratories, Campbell, CA, USA) at a concentration of 1 μg/ml for 1 h. We added kanamycin at 50 μg/ml to each well and incubated the cells for an additional 24 h. We then removed the supernatant, extracted the RNA, and prepared the cDNA library as described above. Oligonucleotide primers specific for *TLR8* and *DUOX2* were constructed (see Table S4 in the supplemental material), and quantitative PCR was carried out using SYBR green and β-actin as a reference gene. We assessed the statistical significance of the gene expression changes using a paired *t* test.

Data availability. The complete database, including the fastq files, from this study has been uploaded for public use and is available at the NIH BioProject page at http://www.ncbi.nlm.nih.gov/bioproject/415406 (BioProject accession number PRJNA415406).

SUPPLEMENTAL MATERIAL

Supplemental material for this article may be found at https://doi.org/10.1128/IAI.00594-17.

SUPPLEMENTAL FILE 1, PDF file, 0.2 MB.

ACKNOWLEDGMENTS

This work was supported by grants from the National Institutes of Health, including the National Institute of Allergy and Infectious Diseases (T32-AI007061 to D.L.B., RO1-AI099243 and AI103055 to J.B.H. and F.Q., AI106878 to E.T.R. and F.Q., K08-AI089721 to R.C.C., and T32-AI007061 to D.L.B.) and the Fogarty International Center, NIH (K43-TW010362 to T.R.B. and D43-TW005572 to R.R. and T.R.B.), and the Robert Wood Johnson Foundation Harold Amos Medical Faculty Development Program to R.C.C.

We are grateful to the study participants and the staff that supported the study. We thank Jennifer Couget, Patricia Della Pelle, and Thomas Diefenbach for their technical assistance.

REFERENCES

1. Ali M, Nelson AR, Lopez AL, Sack DA. 2015. Updated global burden of cholera in endemic countries. PLoS Negl Trop Dis 9:e0003832. https://doi.org/10.1371/journal.pntd.0003832.
2. UNICEF and WHO. 2015. Progress on sanitation and drinking water—2015 update and MDG assessment. UNICEF, New York, NY.
3. Levine MM, Black RE, Clements ML, Cisneros L, Nalin DR, Young CR. 1981. Duration of infection-derived immunity to cholera. J Infect Dis 143:818–820. https://doi.org/10.1093/infdis/143.6.818.
4. Sur D, Lopez AL, Kanungo S, Paisley A, Manna B, Ali M, Niyogi SK, Park JK, Sarkar B, Puri MK, Kim DR, Deen JL, Holmgren J, Carbis R, Rao R, Nguyen TV, Donner A, Ganguly NK, Nair GB, Bhattacharya SK, Clemens JD. 2009. Efficacy and safety of a modified killed-whole-cell oral cholera vaccine in India: an interim analysis of a cluster-randomised, double-blind, placebo-controlled trial. Lancet 374:1694–1702. https://doi.org/10.1016/S0140-6736(09)61297-6.
5. Kabir S. 2014. Critical analysis of compositions and protective efficacies of oral killed cholera vaccines. Clin Vaccine Immunol 21:1195–1205. https://doi.org/10.1128/CVI.00378-14.
6. Harris JB, LaRocque RC, Qadri F, Ryan ET, Calderwood SB. 2012. Cholera. Lancet 379:2466–2476. https://doi.org/10.1016/S0140-6736(12)60436-X.
7. Pulimood AB, Ramakrishna BS, Rita AB, Srinivasan P, Mohan V, Gupta S, Perakath B, Kang G, Chandy G, Balasubramanian KA. 2008. Early activation of mucosal dendritic cells and macrophages in acute Campylobacter colitis and cholera: an in vivo study. J Gastroenterol Hepatol 23:752–758. https://doi.org/10.1111/j.1440-1746.2008.05325.x.
8. Silva TM, Schleupner MA, Tacket CO, Steiner TS, Kaper JB, Edelman R, Guerrant R. 1996. New evidence for an inflammatory component in diarrhea caused by selected new, live attenuated cholera vaccines and by El Tor and Q139 Vibrio cholerae. Infect Immun 64:2362–2364.
9. Mathan MM, Chandy G, Mathan VI. 1995. Ultrastructural changes in the upper small intestinal mucosa in patients with cholera. Gastroenterology 109:422–430. https://doi.org/10.1016/0016-5085(95)90329-1.
10. Flach CF, Qadri F, Bhuiyan TR, Alam NH, Jennische E, Lonnroth I, Holmgren J. 2007. Broad up-regulation of innate defense factors during acute cholera. Infect Immun 75:2343–2350. https://doi.org/10.1128/IAI.01900-06.
11. Qadri F, Bhuiyan TR, Dutta KK, Raqib R, Alam MS, Alam NH, Svennerholm AM, Mathan MM. 2004. Acute dehydrating disease caused by Vibrio cholerae serogroups O1 and O139 induce increases in innate cells and inflammatory mediators at the mucosal surface of the gut. Gut 53:62–69. https://doi.org/10.1136/gut.53.1.62.
12. Shin OS, Uddin T, Citorik R, Wang JP, Della Pelle P, Kradin RL, Bingle CD, Bingle L, Camilli A, Bhuiyan TR, Shirin T, Ryan ET, Calderwood SB, Finberg RW, Qadri F, LaRocque RC, Harris JB. 2011. LPLUNC1 modulates innate immune responses to Vibrio cholerae. J Infect Dis 204:1349–1357. https://doi.org/10.1093/infdis/jir544.
13. Ellis CN, LaRocque RC, Uddin T, Krastins B, Mayo-Smith LM, Sarracino D, Karlsson EK, Rahman A, Shirin T, Bhuiyan TR, Chowdhury F, Khan AI, Ryan ET, Calderwood SB, Qadri F, Harris JB. 2015. Comparative proteomic analysis reveals activation of mucosal innate immune signaling pathways during cholera. Infect Immun 83:1089–1103. https://doi.org/10.1128/IAI.02765-14.
14. Karlsson EK, Harris JB, Tabrizi S, Rahman A, Shlyakhter I, Patterson N, O'Dushlaine C, Schaffner SF, Gupta S, Chowdhury F, Sheikh A, Shin OS, Ellis C, Becker CE, Stuart LM, Calderwood SB, Ryan ET, Qadri F, Sabeti PC, LaRocque RC. 2013. Natural selection in a Bangladeshi population from the cholera-endemic Ganges River Delta. Sci Transl Med 5:192ra186. https://doi.org/10.1126/scitranslmed.3006338.
15. Toma C, Higa N, Koizumi Y, Nakasone N, Ogura Y, McCoy AJ, Franchi L, Uematsu S, Sagara J, Taniguchi S, Tsutsui H, Akira S, Tschopp J, Nunez G, Suzuki T. 2010. Pathogenic Vibrio activate NLRP3 inflammasome via cytotoxins and TLR/nucleotide-binding oligomerization domain-mediated NF-kappa B signaling. J Immunol 184:5287–5297. https://doi.org/10.4049/jimmunol.0903536.
16. Bandyopadhaya A, Chaudhuri K. 2009. Differential modulation of NF-kappaB-mediated pro-inflammatory response in human intestinal epithelial cells by cheY homologues of Vibrio cholerae. Innate Immun 15:131–142. https://doi.org/10.1177/1753425908100454.
17. Bhowmick S, Chatterjee D, Chaudhuri K. 2012. Human epithelial cells stimulated with Vibrio cholerae produce thymic stromal lymphopoietin and promote dendritic cell-mediated inflammatory Th2 response. Int J Biochem Cell Biol 44:1779–1790. https://doi.org/10.1016/j.biocel.2012.06.030.
18. Clements ML, Levine MM, Young CR, Black RE, Lim YL, Robins-Browne RM, Craig JP. 1982. Magnitude, kinetics, and duration of vibriocidal antibody responses in North Americans after ingestion of Vibrio cholerae. J Infect Dis 145:465–473. https://doi.org/10.1093/infdis/145.4.465.
19. Breuer K, Foroushani AK, Laird MR, Chen C, Sribnaia A, Lo R, Winsor GL, Hancock RE, Brinkman FS, Lynn DJ. 2013. InnateDB: systems biology of innate immunity and beyond—recent updates and continuing curation. Nucleic Acids Res 41:D1228–D1233. https://doi.org/10.1093/nar/gks1147.
20. Lipinski S, Till A, Sina C, Arlt A, Grasberger H, Schreiber S, Rosenstiel P. 2009. DUOX2-derived reactive oxygen species are effectors of NOD2-mediated antibacterial responses. J Cell Sci 122:3522–3530. https://doi.org/10.1242/jcs.050690.
21. Cervantes JL, Weinerman B, Basole C, Salazar JC. 2012. TLR8: the forgotten relative revindicated. Cell Mol Immunol 9:434–438. https://doi.org/10.1038/cmi.2012.38.
22. Prendergast AJ, Kelly P. 2016. Interactions between intestinal pathogens, enteropathy and malnutrition in developing countries. Curr Opin Infect Dis 29:229–236. https://doi.org/10.1097/QCO.0000000000000261.
23. Ou G, Rompikuntal PK, Bitar A, Lindmark B, Vaitkevicius K, Wai SN, Hammarstrom ML. 2009. Vibrio cholerae cytolysin causes an inflammatory response in human intestinal epithelial cells that is modulated by the PrtV protease. PLoS One 4:e7806. https://doi.org/10.1371/journal.pone.0007806.
24. Chakraborty DC, Mukherjee G, Banerjee P, Banerjee KK, Biswas T. 2011. Hemolysin induces Toll-like receptor (TLR)-independent apoptosis and multiple TLR-associated parallel activation of macrophages. J Biol Chem 286:34542–34551. https://doi.org/10.1074/jbc.M111.241851.
25. Harrison LM, Rallabhandi P, Michalski J, Zhou X, Steyert SR, Vogel SN, Kaper JB. 2008. Vibrio cholerae flagellins induce Toll-like receptor 5-mediated interleukin-8 production through mitogen-activated protein kinase and NF-kappaB activation. Infect Immun 76:5524–5534. https://doi.org/10.1128/IAI.00843-08.
26. Herrera CM, Crofts AA, Henderson JC, Pingali SC, Davies BW, Trent MS. 2014. The Vibrio cholerae VprA-VprB two-component system controls virulence through endotoxin modification. mBio 5:e02283-14. https://doi.org/10.1128/mBio.02283-14.
27. Khilwani B, Mukhopadhaya A, Chattopadhyay K. 2015. Transmembrane oligomeric form of Vibrio cholerae cytolysin triggers TLR2/TLR6-dependent proinflammatory responses in monocytes and macrophages. Biochem J 466:147–161. https://doi.org/10.1042/BJ20140718.
28. Kariko K, Buckstein M, Ni H, Weissman D. 2005. Suppression of RNA recognition by Toll-like receptors: the impact of nucleoside modification and the evolutionary origin of RNA. Immunity 23:165–175. https://doi.org/10.1016/j.immuni.2005.06.008.
29. Gantier MP, Irving AT, Kaparakis-Liaskos M, Xu D, Evans VA, Cameron PU, Bourne JA, Ferrero RL, John M, Behlke MA, Williams BR. 2010. Genetic modulation of TLR8 response following bacterial phagocytosis. Hum Mutat 31:1069–1079. https://doi.org/10.1002/humu.21321.
30. Sander LE, Davis MJ, Boekschoten MV, Amsen D, Dascher CC, Ryffel B, Swanson JA, Muller M, Blander JM. 2011. Detection of prokaryotic mRNA signifies microbial viability and promotes immunity. Nature 474:385–389. https://doi.org/10.1038/nature10072.
31. Kayagaki N, Warming S, Lamkanfi M, Vande Walle L, Louie S, Dong J, Newton K, Qu Y, Liu J, Heldens S, Zhang J, Lee WP, Roose-Girma M, Dixit VM. 2011. Non-canonical inflammasome activation targets caspase-11. Nature 479:117–121. https://doi.org/10.1038/nature10558.
32. Shenoy AR, Wellington DA, Kumar P, Kassa H, Booth CJ, Cresswell P, MacMicking JD. 2012. GBP5 promotes NLRP3 inflammasome assembly and immunity in mammals. Science 336:481–485. https://doi.org/10.1126/science.1217141.
33. Hayes P, Dhillon S, O'Neill K, Thoeni C, Hui KY, Elkadri A, Guo CH, Kovacic L, Aviello G, Alvarez LA, Griffiths AM, Snapper SB, Brant SR, Doroshow JH, Silverberg MS, Peter I, McGovern DP, Cho J, Brumell JH, Uhlig HH, Bourke B, Muise AA, Knaus UG. 2015. Defects in NADPH oxidase genes NOX1 and DUOX2 in very early onset inflammatory bowel disease. Cell Mol Gastroenterol Hepatol 1:489–502. https://doi.org/10.1016/j.jcmgh.2015.06.005.
34. Grasberger H, Gao J, Nagao-Kitamoto H, Kitamoto S, Zhang M, Kamada N, Eaton KA, El-Zaatari M, Shreiner AB, Merchant JL, Owyang C, Kao JY. 2015.

Increased expression of DUOX2 is an epithelial response to mucosal dysbiosis required for immune homeostasis in mouse intestine. Gastroenterology 149:1849–1859. https://doi.org/10.1053/j.gastro.2015.07.062.
35. David LA, Weil A, Ryan ET, Calderwood SB, Harris JB, Chowdhury F, Begum Y, Qadri F, LaRocque RC, Turnbaugh PJ. 2015. Gut microbial succession follows acute secretory diarrhea in humans. mBio 6:e00381-15. https://doi.org/10.1128/mBio.00381-15.
36. Nelson EJ, Harris JB, Morris JG, Jr, Calderwood SB, Camilli A. 2009. Cholera transmission: the host, pathogen and bacteriophage dynamic. Nat Rev Microbiol 7:693–702. https://doi.org/10.1038/nrmicro2204.
37. Chomczynski P, Sacchi N. 1987. Single-step method of RNA isolation by acid guanidinium thiocyanate-phenol-chloroform extraction. Anal Biochem 162:156–159.
38. Trapnell C, Roberts A, Goff L, Pertea G, Kim D, Kelley DR, Pimentel H, Salzberg SL, Rinn JL, Pachter L. 2012. Differential gene and transcript expression analysis of RNA-seq experiments with TopHat and Cufflinks. Nat Protoc 7:562–578. https://doi.org/10.1038/nprot.2012.016.
39. Kim D, Pertea G, Trapnell C, Pimentel H, Kelley R, Salzberg SL. 2013. TopHat2: accurate alignment of transcriptomes in the presence of insertions, deletions and gene fusions. Genome Biol 14:R36. https://doi.org/10.1186/gb-2013-14-4-r36.
40. Kramer A, Green J, Pollard J, Jr, Tugendreich S. 2014. Causal analysis approaches in Ingenuity Pathway Analysis. Bioinformatics 30:523–530. https://doi.org/10.1093/bioinformatics/btt703.
41. Murley YM, Behari J, Griffin R, Calderwood SB. 2000. Classical and El Tor biotypes of Vibrio cholerae differ in timing of transcription of tcpPH during growth in inducing conditions. Infect Immun 68:3010–3014. https://doi.org/10.1128/IAI.68.5.3010-3014.2000.